Available online at www.sciencedirect.com
SCIENCE DIRECT®
Chemical Physics 322 (2006) 360–365
Chemical Physics
www.elsevier.com/locate/chemphys

Cluster-assisted multiple ionization of methyl iodide by a nanosecond laser: Influence of laser intensity on the kinetic energy and peak profile of multicharged ions

Lihua Wen, Haiyang Li *, Xiaolin Luo, Dongmei Niu, Xue Xiao, Bin Wang, Feng Liang, Keyong Hou, Shiyong Shao

Dalian Institute of Chemical Physics, Analytical Chemistry, 102 Group, 457 Zhongshan Road, Chinese Academy of Sciences, Dalian, Liaoning 116023, PR China
Key Laboratory of Environmental Optics and Technology, Anhui Institute of Optics and Fine Mechanics, Chinese Academy of Sciences, Hefei 230031, PR China

Received 10 March 2005; accepted 12 September 2005
Available online 30 September 2005

Abstract

The dependences of kinetic energies and peak profiles of multicharged ions of I^{q+} ($q = 2$–3) and C^{2+} on the laser intensity have been studied in detail by time-of-flight mass spectrometry, those multicharged ions are produced by irradiation of methyl iodide cluster beam with a nanosecond 532 nm Nd-YAG laser. Our experiments show that the kinetic energies released of multicharged ions increase linearly with the laser intensity in the range of 3×10^9–2×10^{11} W/cm^2. The peaks of multicharged ions are split to forward ions and backward ions, and the ratio of the backward ions to forward ions decreases exponentially with laser intensity. The decreasing of backward ions is probably due to Coulomb scattering by the heavier I^+ ions when they turn around through the laser focus point. The linear dependence of kinetic energy of multicharged ions on laser intensity is interpreted by the ionization mechanism, in which the laser induced inverse bremsstrahlung heating of electron is the rate-limiting step.

Keywords: Methyl iodide; Multiple ionization; Cluster; Space charge effect

1. Introduction

As the bridge systems between isolated molecules and the condensed phase, cluster in laser field has been extensively studied in recent years [1–18]. When atomic and molecular clusters are used as the target of the intense laser beams, the phenomena occurring are much distinct from those of isolated molecules, for example, Coulomb explosion (CE). When the repulsive energy overcomes the total cohesive energy of the cluster, the highly ionized cluster explodes into atomic and molecular fragments with higher charge states and larger kinetic energies released (KER) than those from isolated molecule systems. In general, the KER of the atomic ions generated from CE of isolated molecule systems are only tens of electron volt, while the irradiation of a cluster of 10^3–10^6 atoms could generate fast electrons of a few keV and highly charged ions as high as +40 with KER up to MeV [5–7].

Castleman and co-workers reported the Coulomb explosion of methyl iodide clusters irradiated by a 128 fs laser at the intensity of 10^{15} W/cm^2. When methyl iodide beam seeded in argon was irradiated by a laser at wavelength of 795 nm, C^{q+} ($q = 1$–4) and I^{q+} ($q = 1$–15) were observed, while C^{q+} ($q = 1$–4) and I^{q+} ($q = 1$–7) were detected by irradiation of the harmonic output of the laser at 397 nm. The mechanism of the Coulomb explosion process was

* Corresponding author. Tel.: +86 411 84379509; fax: +86 411 84379517.
E-mail addresses: hli@dicp.ac.cn, hli@aiofm.ac.cn (H. Li).

0301-0104/$ - see front matter © 2005 Elsevier B.V. All rights reserved.
doi:10.1016/j.chemphys.2005.09.006

not clearly declared; it may be some combination of the ionization ignition model (IIM) and coherent electron motion model (CEMM) [8,9]. Recently, we reported the productions of C^{2+} and I^{q+} ($q = 2$–3) in laser ionization of methyl iodide seeded in argon by a 25 ns, 532 nm Nd-YAG laser at intensity only about 10^{11} W/cm^2. The multicharged ions were observed only in the dense portion of the pulsed molecular beam, where the concentration of clusters was high. A simple illustrative model was proposed to explain the phenomenon of cluster-assisted multiple ionization (CAMI) in the nanosecond laser filed [10]. The multicharged ion is produced by recolliding ionization of energetic electrons, which obtain energy via inverse bremsstrahlung (IBS) absorption from the laser field.

However, there are still many questions about CAMI process need further study, such as: (1) The KER of multicharged ions measured at various laser intensity differed by almost two-orders in the literature [8–10], what is the relationship between KER and the laser intensity? (2) Does the ion intensity in the mass spectra reflect the real relative intensity of different ions at birth? (3) In our previous report [10], we found that the intensity of the backward peak of multicharged ions was always smaller than that from simulation, what is the reason? These are the motivations of present study.

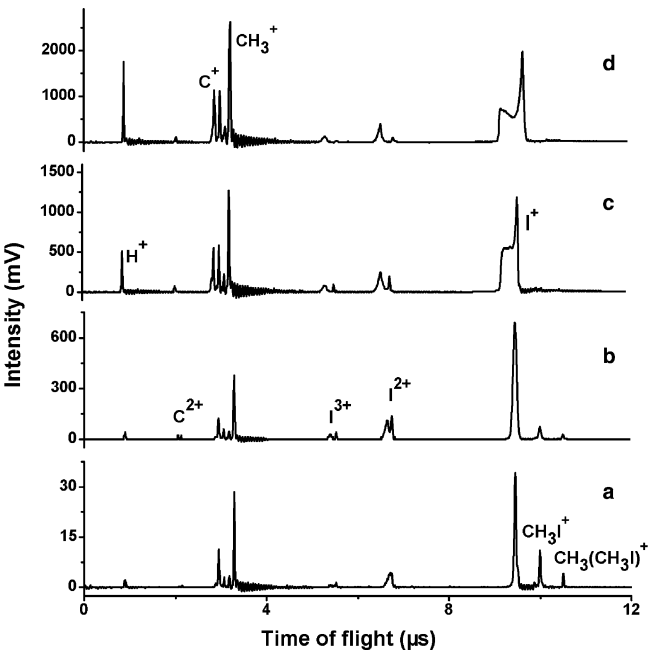

Fig. 1. Time-of-flight mass spectra for He seeded CH_3I beam at various 532 nm laser intensities. (a) 4.4×10^9 W/cm^2, (b) 1.9×10^{10} W/cm^2, (c) 6.7×10^{10} W/cm^2, and (d) 1.4×10^{11} W/cm^2. Even at the threshold intensity for detection, multicharged ions C^{2+}, I^{2+}, I^{3+} are observed. At higher intensity, the multicharged ions show significant increase of kinetic energy released.

2. Experimental

The apparatus used in this study was a home-made linear Wiley–Mclaren two-stage time-of-flight mass spectrometer (TOFMS), which has been described in detail elsewhere [10,11]. Briefly, methyl iodide seeded in helium of 0.3 MPa was introduced to the vacuum chamber via a pulsed nozzle (General Valve Corporation, $\phi = 0.5$ mm) and then passed through a skimmer ($\phi = 3$ mm) to be ionized. The interaction region of the laser with the pulsed molecular beam was situated about 130 mm downstream of the pulsed nozzle. The pressure in the ionization chamber was about several 10^{-4} Pa under a sample inlet frequency of 10 Hz. The laser system was a commercially available Nd-YAG laser (Spectron SL803, 100 mJ at 532 nm, 25 ns). The intensity of laser at focus point used in the experiment was 3×10^9–2×10^{11} W/cm^2. The produced ions were first accelerated by the extraction electric field, and then detected by the dual microchannel plates (MCP, $\phi = 30$ mm) after 250/500 mm field-free flight. The total voltage on the extraction plate is 2800 V. The time-of-flight mass spectrum was recorded on a digital oscilloscope (Tektronix, TDS224) after averaging for 128 laser shots. The CH_3I, purchased from Shanghai Chemical Reagent Corporation, had a purity of 98.5%. The carrier gases (Nanjing Special Gases Corporation) had a purity of 99.99%.

3. Results and analysis

Fig. 1 shows the time-of-flight mass spectra obtained by irradiating the 532 nm laser on methyl iodide beam at different laser intensities from 4.4×10^9 to 1.4×10^{11} W/cm^2. As we can see from Fig. 1(a), both single charged ions and multicharged ions appear in the spectrum. The domain single charged ions are H^+, C^+, CH_3^+, I^+ and weak CH_3I^+, $(CH_3I)CH_3^+$ ions, which are common ionic products of multiphoton ionization and dissociation (MPID) [13]. The multicharged ions C^{2+}, I^{2+} and I^{3+} appear even at the threshold detection intensity of 3×10^9 W/cm^2, and the charge state distribution of multicharged ions does not change apparently while increasing the laser intensity 30 times from 4.4×10^9 W/cm^2 in Fig. 1(a) to 1.4×10^{11} W/cm^2 in Fig. 1(d). The peak profiles of C^{2+}, I^{2+} and I^{3+} ions split to forward and backward peaks, as shown in Fig. 1(a)–(d), and the time interval Δt between the backward and forward ion increases with the increase of laser intensity. The peak splitting of multicharged ions indicates that Coulomb explosion takes place in the ionization process. The KER can be calculated using Eq. (1),

$$E_{(\mathrm{KER})} = \frac{q^2 e^2 F^2 \Delta t^2}{8m}, \tag{1}$$

where q is the charge number of the ion, e the elemental charge, F the static electric field of the extraction region (700 V/cm), m the mass of the ion. Fig. 2 shows the KERs of C^{2+}, I^{2+} and I^{3+} ions versus the laser energy. As we can see, the KERs increase almost linearly with the increase of laser energy. The KER increasing rates of I^{2+} and I^{3+} are determined as 3.6 ± 0.2, 5.8 ± 0.2 eV/mJ, respectively, in the energy range of 2–45 mJ/pulse.

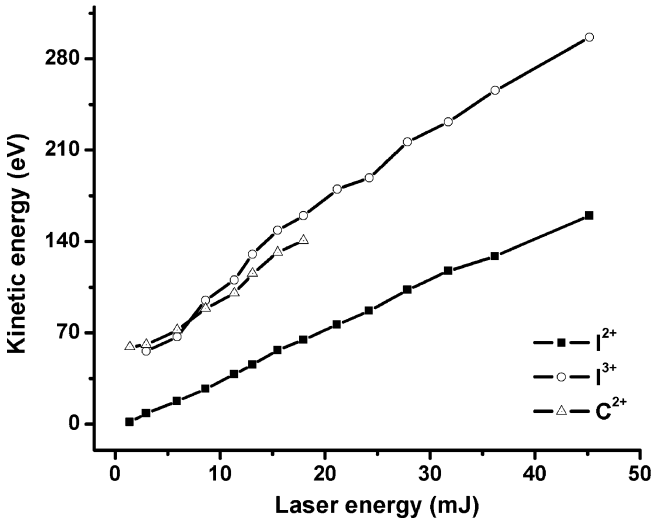

Fig. 2. The kinetic energies released of C^{2+}, I^{2+} and I^{3+} ions as a function of the laser energy.

Fig. 3 shows the integrated ion intensities of I^{q+} ($q = 1$–3) ions versus laser intensity. The integrated ion signal of I^{q+} ($q = 1$–3) increases as $I^{2.3\pm0.1}$ with laser intensity I, when $I < 2.7 \times 10^{10}$ W/cm^2; When $I > 2.7 \times 10^{10}$ W/cm^2, the integrated ion signal of I^+ increases as $I^{0.7}$ with laser intensity, while the intensities of I^{2+} and I^{3+} do not increase distinctly.

We are interested to know what cause the ion intensities do not increase apparently with the laser intensity after laser intensity exceeds 2.7×10^{10} W/cm^2. The splitting peak profile from forward and backward ions come from the limited acceptance angle for ions with large KER, as the angle distribution of the ions was determined to be isotropic by rotating the polarization direction of the laser from parallel to perpendicular to the flight axis [10]. Since the KERs of multicharged ions increase linearly with laser intensity, we guess that the acceptance angle for ions with higher KER becomes smaller, which cause the ion integrated intensities of I^{2+} and I^{3+} do not increase with laser apparently after $I > 2.7 \times 10^{10}$ W/cm^2. In order to confirm the effect of the acceptance angle, mass spectra were taken using two flight tubes with length (a) 500 mm, and (b) 250 mm under the same beam and laser condition, as shown in Fig. 4(a) and (b). The intensity ratio of $I_{250}(CH_3^+)/I_{500}(CH_3^+)$ in Fig. 4 is about 2.2, while the intensity ratio of forward I^{2+}, i.e. $I_{250}(I_f^{2+})/I_{500}(I_f^{2+})$ is 3.1. We also calculate the intensity ratio of different ions at two lengths of flight tube by assuming the KER has a distribution of Gaussian. The calculated ratio is $I_{250}(CH_3^+)/I_{500}(CH_3^+) = 2.0$, and $I_{250}(I_f^{2+})/I_{500}(I_f^{2+}) = 3.5$, respectively. From simulation, we also know that 56% of CH_3^+ with KER less than 1 eV can be detected, while only 1% of I^{2+} can reach the detector when its most probable KER reaches 140 eV. In short, the intensity of multicharged ions with large kinetic energy from Coulomb explosion should be much stronger than that of singly charged ions with small kinetic energy from MPI in our spectra.

Another interesting feature about the peak profiles of multicharged ions is that the intensity ratio of backward and forward ions decreases dramatically with the increase of laser intensity. For example, the peak heights of backward and forward ions are almost same at threshold detection laser intensity in Fig. 1(a), while the backward peak of C^{2+} ions gradually disappear when the laser intensity exceeds 6.7×10^{10} W/cm^2, as shown in Fig. 1(c). Fig. 5 shows a plot of the intensity ratio of backward and forward ions of I^{2+}, I^{3+} and C^{2+} as a function of laser intensity. The ratio decreases exponentially with laser intensity, and the backward C^{2+} ion decreases more quickly than the backward I^{2+} and I^{3+} ions.

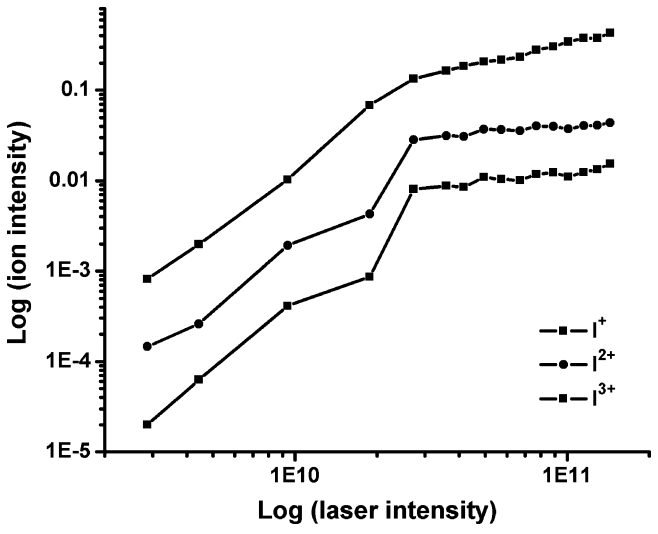

Fig. 3. A plot of the logarithm of the integrated intensities of I^+, I^{2+} and I^{3+} ions as a function of the logarithm of the 532 nm laser intensity.

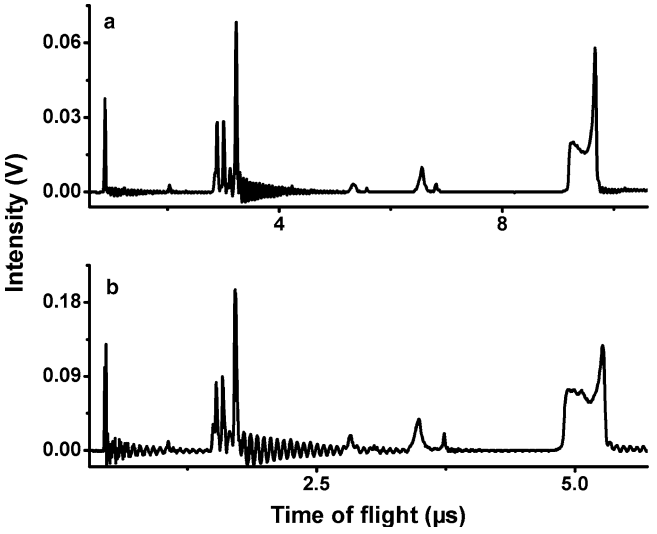

Fig. 4. Time-of-flight mass spectra taken using field-free flight tube with different length. (a) 500 mm, (b) 250 mm, respectively. Laser intensity: 1.2×10^{11} W/cm^2.

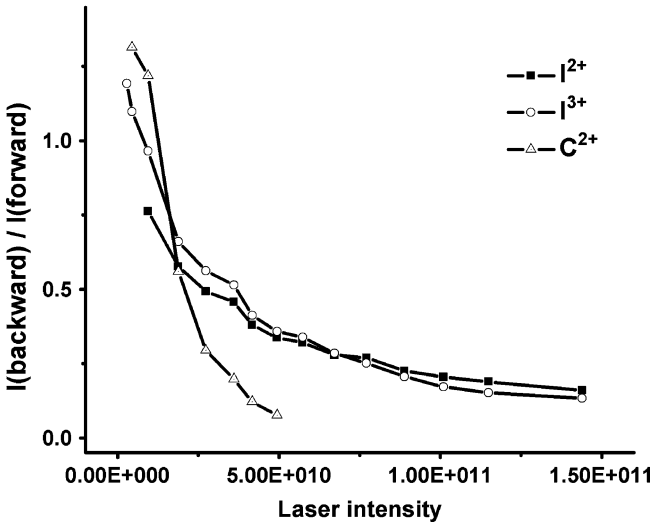

Fig. 5. Intensity ratio of the backward and the forward ions as a function of the laser intensity.

4. Discussion

4.1. Kinetic energies released of multicharged ions

The mechanism of cluster assisted multiple ionization process at the intensity of 10^{10}–10^{11} W/cm^2 has been discussed in detail elsewhere [10,12]. First, the neutral cluster absorbs several photons to be ionized, which was speculated to consist of nearly 10^3 molecules per cluster according to the Hagena parameter [19]. Some of electrons maybe caged in the sizeable cluster due to: (a) the rebound from the solid-dense neutral atoms or molecules in neighborhood; and (b) Coulomb attraction of the ion core. These caged electrons are heated by the electromagnetic field through inverse bremsstrahlung (IBS) absorption while collision with the neutral particles or ions. When the electrons gain enough energy to surpass the corresponding ionization potential, electron-impact ionization (EI) can take place. These heating and ionization processes circulate until the multicharged molecular ions explode to pieces by the increasing Coulomb repelling forces.

Recently, Last and Jortner [20,21] have made detailed description of the interaction of Xe and CD_4 clusters with femtosecond laser pulses of intensity of 10^{16}–10^{19} W/cm^2. They draw a conclusion that the barrier suppression ionization (BSI) mechanism is the vital process, while the electron-impact ionization (EI) only takes a minor role in the production of the highly charged ions, and the ratio of the EI to the BSI decreases with the augmenting of laser intensity, for example, from 13% at 10^{16} W/cm^2 decreases to 6% at 10^{18} W/cm^2 in CD_4 clusters. But in present work, owing to the increasing of KERs and the intensity of the multicharged ions with increasing the laser intensity, an opposite conclusion could be drawn that, at such low laser intensity, heating of electron through IBS and EI process tend to much more violent at higher laser intensity, and BSI contributes much less to the ionization even at the highest laser intensity due to the Keldysh parameter [22]. The heating of electron by IBS plays a controlling role in the long, e.g., nanosecond laser pulse, and this heating may last almost in the whole laser pulse, which leads to the high energy of the electron.

The heating rate of the electron (disregarding the energy losses in the collisions) can be estimated from the following equation [23–25]:

$$\frac{d\varepsilon}{dt} = \Delta E \times (v_{ei} + v_{en}), \tag{2}$$

where v_{ei} is the electron–ion collision frequency, v_{en} is the electron–neutral collision frequency. ΔE is the average energy absorbed by the electron in a single collision with ions or neutral atoms and molecules.

$$\Delta E \sim 2U_p = 1.86 \times 10^{-13} I\lambda^2 \text{ (eV)}, \tag{3}$$

where U_p is the ponderomotive potential of the radiation field and refers to the quiver motion of the electron in the oscillating field, I is the laser intensity in W/cm^2, λ is the laser wavelength in μm. The electron-ion/neutral collision frequency inside a cluster is on the order of 10^{14} Hz due to near-liquid density ($10^{21\sim22}$/cm^3), the electron-heating rate can reach 10^2–10^3 eV/ns, so it takes only tens of picoseconds to heat an electron to surpass the ionization potential, and induce impact ionization. Multiphoton ionization (MPI) is only an ignition step but not a controlling step of the whole ionization process, the final charge distribution and ion yield dependent on the heating rate of the electron inside a cluster.

The KER for a specific kind of ion on the average is proportional to the sum of repelling energy between the ion and all other ions in a cluster, i.e., KER of ion j should increase linearly with its charge Q_j, and increase linearly with the total number of ions in a cluster. The ionization yield of a cluster depends on the electron-heating rate, and the later has a linear relation with laser intensity, this can possibly account for the linear dependence of KERs on laser energy shown in Fig. 3. The experimental ratio of KER increasing rate with laser energy of I^{3+}/I^{2+} is $5.8/3.6 = 1.6 \pm 0.1$, which agrees quite well with the theoretical value 3/2, and this strongly supports the above analysis.

4.2. Space charge effects on the peak profiles

In most of CE experiment studied by a time-of-flight mass spectrometer, the intensity of backward ions is generally smaller than that of forward ions [8–11]. There are several factors attributed to this phenomenon, for example: (1) some backward ions, due to large kinetic energy, cannot be stopped by the spectrometer and annihilate on the repeller plate; (2) the acceptance angle for the backward ions is smaller than the acceptance angle for the forward ions because the backward ions spend a turn around time additionally. However, even if the above two factors have been carefully considered in the simulation program, the

experimental intensity of backward ions is still much smaller than that simulated intensity, especially at higher laser intensity. Fig. 6 shows a plot of experimental and simulated peak profiles of I^{3+} at various laser intensities. As we can see, the experimental and simulated agree quite well at laser intensity less than 2.4×10^{10} W/cm^2 as shown in Fig. 6 (a), but the discrepancy between the experimental and simulated become obvious when laser intensity increases to 4.2×10^{10} W/cm^2. The I_b^{exp}/I_b^{simu} of I^{3+} ions decreases from 1/2 in Fig. 6(b) to 1/7 in Fig. 6(d).

There are a large number of neutral and ionic species in the beam, so the backward ions encounter more collisions with the particles when they turn around and pass the ionization focus point. The backward ions decrease exponentially with laser intensity while the molecular beam condition is kept the same. We think that the Coulomb repulsion of the high density I^+ cloud with the multicharged ions, i.e., space-charge effect, could make some backward ions change their trajectories off the detector [26–30], while the multicharged ion-neutral collision make minor contribution to the loss of backward ions. The magnitude of ionic trajectory changed dependents on the charge and mass of the repelling ions, and lighter ion loss more signal while pass the heavy ion cloud. The backward C^{2+} ions are easier affected by the dense I^+ cloud than I^{2+} and I^{3+} ions, as the mass of C atom is ten times smaller than that of I atom. In summary, space charge repelling has a strong effect on the peak profiles in laser-cluster ionization experiments, the backward ions may totally disappear in the mass spectrum, this could make some confusion in assigning and interpreting the ion peaks, a comparison of the peak profiles taken at various laser intensity are highly needed when using very intense laser.

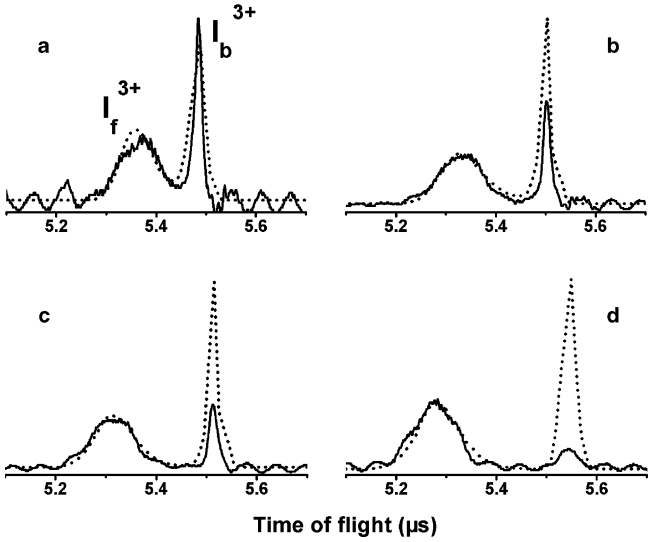

Fig. 6. The experimental and simulated peak profiles of I^{3+} at the laser intensity of: (a) 2.4×10^{10} W/cm^2, (b) 4.2×10^{10} W/cm^2, (b) 6.7×10^{10} W/cm^2, (b) 1.4×10^{11} W/cm^2. The backing pressure of seeding gas is 0.3 MPa helium gas. Solid lines are experimental peak profiles and dot lines simulated.

5. Conclusions

In conclusion, the laser intensity influences on the intensities and the kinetic energies of multicharged ions arising from cluster assistant multiple ionization and Coulomb explosion of methyl iodide cluster by a nanosecond laser at 532 nm have been studied in detail. Multiply charged ions are generated even at the detection threshold laser intensity. The good linear dependence of KER of multicharged ions on laser intensity can attribute to the rate-limiting step in the production of multicharged ions, i.e., the electron-heating rate inside a cluster via IBS absorption, which is proportional to laser intensity. In our experiment, the acceptance angle and space charge effect are two important factors affecting the ion intensity and peak profile in the mass spectrum, and only very small part of the produced multicharged ions from CE can be detected in intense laser ionization.

Acknowledgements

The work was partly supported by the NSF of China, 863 High Technology Program, and the Center for Computational Science, Hefei Institute of Physical Sciences. The authors thank Professor Guohe Sha for fruitful discussion.

References

[1] H. Wabnitz, L. Bittner, A.R.B. de Castro, R. Döhrmann, P. Gürtler, T. Laarmann, W. Laasch, J. Schulz, A. Swiderski, K. von Haeften, T. Möller, B. Faatz, A. Fateev, J. Feldhaus, C. Gerth, U. Hahn, E. Saldin, E. Schneidmiller, K. Sytchev, K. Tiedtke, R. Treusch, M. Yurkov, Nature (London) 420 (2002) 482.
[2] C. Rose-Petruck, K.J. Schafer, K.R. Wilson, C.P.J. Barty, Phys. Rev. A. 55 (1997) 1182.
[3] A. McPherson, T.S. Luk, B.D. Thompson, K. Boyer, C.K. Rhodes, Appl. Phys. B. 57 (1993) 337.
[4] A. McPherson, B.D. Thompson, A.B. Borisov, K. Boyer, C.K. Rhodes, Nature 370 (1994) 631.
[5] T. Ditmire, T. Donnelly, R.W. Falcone, M.D. Perry, Phys. Rev. Lett. 75 (1995) 3122.
[6] T. Ditmire, J.W.G. Tisch, E. Springate, M.B. Mason, N. Hay, R.A. Smith, J.P. Marangos, M.H.R. Hutchinson, Nature (London) 386 (1997) 54.
[7] Y.L. Shao, T. Ditmire, J.W.G. Tisch, E. Springate, J.P. Marangos, M.H.R. Hutchinson, Phys. Rev. Lett. 77 (1996) 3343.
[8] J.V. Ford, Q. Zhong, L. Poth, A.W. Castleman Jr., J. Chem. Phys. 110 (1999) 6257.
[9] J.V. Ford, L. Poth, Q. Zhong, A.W. Castleman Jr., Int. J. Mass Spectrom. 192 (1999) 327.
[10] X. Luo, D. Niu, X. Kong, L. Wen, F. Liang, K. Pei, B. Wang, H. Li, Chem. Phys. 310 (2005) 17.
[11] X. Kong, X. Luo, D. Niu, H. Li, Chem. Phys. Lett. 388 (2004) 139.
[12] D. Niu, H. Li, F. Liang, L. Wen, X. Luo, B. Wang, K. Hou, X. Zhang, Chem. Phys. Lett. 403 (2005) 218.
[13] Y.-K. Choi, Y.-M. Koo, K.-W.J. Jung, Photochem. Photobiol. A: Chem. 127 (1999) 1.
[14] J. Purnell, E.M. Snyder, S. Wei, A.W. Castleman Jr., Chem. Phys. Lett. 229 (1994) 333.
[15] E.M. Snyder, S.A. Buzza, A.W. Castleman Jr., Phys. Rev. Lett. 77 (1996) 3347.
[16] T. Ditmire, J. Zweiback, V.P. Yanovsky, T.E. Cowan, G. Hays, K.B. Wharton, Nature 398 (1999) 489.

[17] H. Honda, E. Miura, K. Katsura, E. Takahashi, K. Kondo, Phys. Rev. A. 61 (2000) 023201.
[18] M. Lezius, S. Dobosz, D. Normand, M. Schmidt, Phys. Rev. Lett. 80 (1998) 261.
[19] O.F. Hagena, W. Obert, J. Chem. Phys. 56 (1972) 1793.
[20] I. Last, J. Jortner, J. Chem. Phys. 120 (2004) 1336.
[21] I. Last, J. Jortner, J. Chem. Phys. 120 (2004) 1348.
[22] V. Keldysh, Sov. Phys. JEPT. 20 (1965) 1307.
[23] T. Ditmire, T. Donnelly, A.M. Rubenchik, R.W. Falcone, M.D. Perry, Phys. Rev. A. 53 (1996) 3379.
[24] V.P. Krainov, M.B. Smirnov, Phys. Rep. 370 (2002) 237.
[25] M. Lezius, S. Dobosz, D. Normand, M. Schmidt, J. Phys. B. 30 (1997) L251.
[26] C. de Lisio, C. Altucci, R. Bruzzese, T. Di Palma, S. Solimeno, N. Spinelli, V. Tosa, J. Phys. B. 25 (1992) 4781.
[27] C. Girardeau-Montaut, J.P. Girardeau-Montaut, Phys. Rev. A. 44 (1991) 1409.
[28] K.A. Cox, C.D. Cleven, R.G. Cooks, Int. J. Mass Spectrom. Ion Processes 144 (1995) 47.
[29] P.K. Taylor, I.J. Amster, Int. J. Mass Spectrom. 222 (2003) 351.
[30] J.W. Olesik, M.P. Dziewatkoski, J. Am. Soc. Mass Spectrom. 7 (1996) 362.